Organic & Biomolecular Chemistry

PAPER

View Article Online
View Journal | View Issue

Cite this: *Org. Biomol. Chem.*, 2014, **12**, 2263

Design, synthesis and properties of artificial nucleic acids from (*R*)-4-amino-butane-1,3-diol†

Pengfei Li,‡[a] Jingjing Sun,‡[a] Meng Su,[a] Xiaogai Yang[b] and Xinjing Tang*[a]

Received 17th November 2013,
Accepted 30th January 2014

DOI: 10.1039/c3ob42291g

www.rsc.org/obc

A new artificial nucleic acid analogue, (*R*)-Am-BuNA, was developed with a simplified acyclic (*R*)-4-amino-butane-1,3-diol phosphodiester backbone. Phosphoramidite monomers of (*R*)-Am-BuNA were incorporated into DNA oligonucleotides (ODNs) and G-quadruplexes. Their thermal stability, conformation change and biological stability were further investigated using UV-melting, circular dichroism (CD) and gel electrophoresis. The results suggested that thermal stability of the duplexes of (*R*)-Am-BuNA modified ODNs and their complementary ODN is highly dependent on the substitution position. Substitution of thymidine at the 7th position in a thrombin-binding DNA aptamer (TBA) results in a slight increase in T_m with no effect on quadruplex conformation on the CD spectrum in comparison to that of the natural G-quadruplex. Further enzymatic experiments with fetal bovine serum (FBS) and snake venom phosphodiesterase (SVPDE) indicated that only single replacement of a (*R*)-Am-BuNA modified nucleobase greatly inhibited oligonucleotide degradation, which shows their promising applications as capping nucleotides in nucleic acid drugs.

Introduction

Nucleic acids are important biological molecules for storing genetic information as well as regulating biological functions. Artificial nucleic acids with modifications of nucleosides and/or backbone have been developed to mimic natural nucleic acids and have shown broad applications such as diagnostics, therapeutic agents and building blocks for constructing nanostructures.[1] Among many artificial nucleic acids, modifications of oligonucleotide sugar rings have also been extensively investigated to improve the binding ability for target oligonucleotides and the resistance to nucleases.[2]

One of the directions was focused on artificial nucleotide mimics without sugar rings. With pseudopeptide linkage instead of a phosphodiester backbone, peptide nucleic acids (PNA)[3] show remarkably strong hybridization with its complementary DNA or RNA due to a non-charged backbone and resistant to various proteases and nucleases.[4] However, low solubility and poor cellular uptake of PNAs limit their applications if no further modifications are applied.[5] Together with PNAs, unlocked nucleic acids (UNAs), as the most studied acyclic analogues of nucleotides, were developed and optimized for the applications of oligonucleotide-based technology.[6] UNAs have a highly flexible scaffold with removing the C2′–C3′ bond in contrast with natural ribonucleotides. Nucleic acids with UNA modification lead to the decrease of duplex thermal stability in both DNA and RNA.[7] The destabilization of the UNA modified-duplex limits its use in antisense oligonucleotides in some way, but UNA modified siRNA has shown broad potential applications due to its low toxicity and reduction of off-target effects.[8] In addition, Benner *et al.* reported an acyclic nucleotide analogue from glycerol derived building blocks.[9] Oligonucleotides modified with this nucleotide analogue formed less stable duplexes with their complementary sequences.[10] To search for more artificial nucleic acids, many new acyclic nucleotides have been developed. The Meggers group disclosed a new nucleic acid analogue–glycol nucleic acid (GNA) with structural simplicity and atom economy.[11] GNA maintains the canonical Watson–Crick base pairing combined with an acyclic three-carbon propylene glycol phosphodiester backbone. Propylene glycol nucleosides constitute the most simplified possible building blocks for a phosphodiester-bond-containing nucleic acid. In addition, the thermal stability of the GNA duplex significantly surpasses DNA and RNA duplexes with the same sequence. Thermodynamic parameters of duplex formation indicate that the enthalpy of GNA duplex formation is less favorable than that of DNA duplex formation, but its entropy is significantly favorable.[12] Further crystal structure of GNA showed the existence

[a]*State Key Laboratory of Natural and Biomimetic Drugs, School of Pharmaceutical Sciences, Peking University, Beijing 100191, China, and State Key Laboratory of Drug Research, Shanghai Institute of Materia Medica, Chinese Academy of Sciences, Shanghai 201203, China. E-mail: xinjingt@bjmu.edu.cn; Tel: +86-010-82805635*
[b]*Department of Chemical Biology, School of Pharmaceutical Sciences, Peking University, Beijing 100191, China*

†Electronic supplementary information (ESI) available: NMR, ESI-Mass and additional figures and tables are provided. See DOI: 10.1039/c3ob42291g

‡These authors have equal contributions.

of the large average slide (around 3.4 Å) between neighboring base pairs in (*S*)-GNA duplex itself due to a large backbone-base inclination compared with B-DNA.[13] Even though GNA can form a more stable duplex itself, its duplex with DNA or RNA oligonucleotides is still less stable than the duplex of DNA or RNA oligonucleotide themselves. Recently Asanuma *et al.* reported two artificial nucleic acid analogues (TNA and SNA) based on acyclic threoninol and serinol scaffolds. TNA and SNA contained three carbons between two phosphates instead of two carbons for GNA. In addition, SNA could form a relative stable duplex with its target DNA or RNA irrespective of the sequence.[14]

In TNA and SNA analogues, an amide bond is formed as a linkage between a nucleobase and the backbone instead of direct attachment of a nucleobase to the backbone. When we first started to develop artificial nucleic acids, (*S*)-3-amino-1,2-propanediol and (*R*)-4-amino-butane-1,3-diol were chosen as scaffolds to demonstrate the effect of the length of the backbone unit on thermal stability of their duplexes. In the design of each scaffold monomer, the amine group was attached with a nucleobase through an amide bond formation, while the primary hydroxyl group was coupled with trityl group and the secondary hydroxyl group was used to form a phosphoramidite. These artificial nucleotides were efficiently incorporated into oligonucleotides by a DNA solid phase synthesizer. Oligonucleotides with the incorporation of these monomers contained the extended distance of nucleobases/backbone and two or three carbons between two backbone phosphates. Further studies of the formation of duplexes and quadruplexes, and their enzymatic stability were investigated.

Results and discussion

Rational design of artificial nucleic acids from (*R*)-4-amino-butane-1,3-diol ((*R*)-Am-BuNA)

According to the reported nucleic acid analogues, we are devoted to the design and evaluation of novel artificial nucleic acids, which could have potential applications in pharmaceutical sciences. Since the phosphodiester bonds in nucleic acids play an important role in biological functions of nucleic acids, which guarantees the solubility in water and allows organisms to adapt biophysical conditions, we maintained the phosphodiester bond for our artificial nucleic acids. In addition, the acyclic backbone was based on six-bond-per-backbone units of vicinal phosphodiester groups similar to DNA and RNA with the purpose of maintaining the distance between conventional Watson–Crick or Hoogsteen base-pairings. Based on the structures of DNA or RNA, the scaffold of 1,3-butanediol with three carbon atoms and six-bond-per-backbone units was implemented in (*R*)-Am-BuNA (Scheme 1). In addition, a chiral carbon is introduced in the acyclic monomer with the same conformation as 3′-C in ribose. And nucleobases were coupled to the amine group on a phosphate backbone through an amide bond linkage based on the feasibility of synthesis and the stability of anti-nucleases. Two model

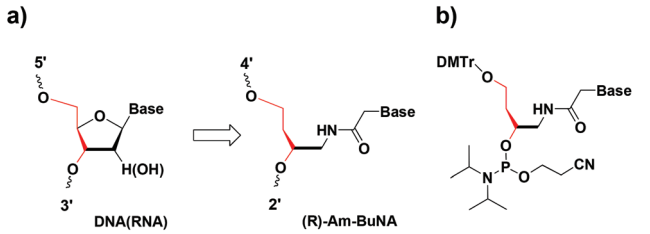

Scheme 1 (a) Structures of DNA (RNA) and (*R*)-Am-BuNA. (b) Phosphoramidite of (*R*)-Am-BuNA.

sequences were then chosen for the incorporation of (*R*)-Am-BuNA. One sequence (CACACCTTGCCATCG) is an antisense oligonucleotide for matrix metalloproteinase 2 (mmp-2),[15] and the other sequence (GGTTGGTGTGGTTGG) is an anti-thrombin-binding aptamer (TBA), a G-rich oligonucleotide that can form a G-quadruplex aptamer.[16]

Synthesis of (*R*)-Am-BuNA phosphoramidite building blocks

For constructing the (*R*)-4-amino-butane-1,3-diol backbone, ethyl-(*R*)-4-chloro-3-hydroxybutanoate was used as the starting material as shown in Scheme 2. This compound was converted to the diol compound **B1** through reduction with sodium borohydride complex in THF in the quantitative yield. With the treatment of sodium azide in DMF, azide compound **B1-1** was obtained with less than 20% yield and its purification was difficult. Then the diol compound **B1** reacted with 1.1 equivalence of DMT chloride to afford the compound **B2**. **B2-1** was prepared through an azide S_N2 reaction, while the yield was still not satisfactory. Finally, another route was chosen. With the treatment of 5 M sodium hydroxide solution at room temperature, epoxy compound **B3** was obtained from **B2** in the quantitative yield. DMTr-epoxy compound **B3** was subject to ring opening with ammonia-saturated methanol solution to afford the scaffold, DMTr-(*R*)-4-aminobutane-1,3-diol (**B4**) with 70% yield over four steps. In comparison, we also synthesized another set of artificial nucleic acid analogues based on (*S*)-3-amino-1,2-propanediol as a scaffold (see ESI S2† for detail).

In order to attach nucleobases to the acyclic backbone *via* amide linkage, an acetic modification of nucleobases was carried out as shown in Scheme 2 and Scheme S1.† Ethyl-3-(3-dimethylaminopropyl) carbodiimide hydrochloride (EDC-Cl) and *N*-hydroxybenzotriazole (HOBt) were used as coupling reagents for the amide bond formation between four acetic-nucleobases and acyclic scaffold **B4**. After purification, the designed products **A1**/**G1**/**C1**/**T1** were obtained with 60–84% yields. Under anhydrous and anaerobic conditions, four phosphoramidite monomers **A2**/**G2**/**C2**/**T2** for solid phase synthesis were obtained and were further characterized with ^{1}H-NMR and ^{31}P-NMR spectra (Scheme 3).

Phosphoramidite monomers **A2**/**G2**/**C2**/**T2** were then used to synthesize oligonucleotides (see Table 1) by an automated solid-phase DNA synthesizer under the same conditions as natural nucleoside phosphoramidite monomers with similar coupling efficiencies. Cleavage and deprotection of the

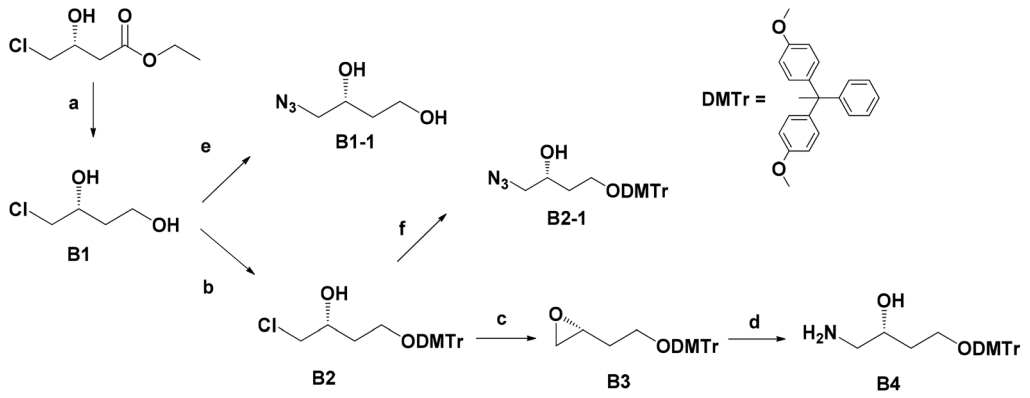

Scheme 2 Synthesis of (*R*)-4-aminobutane-1,3-diol. (a) $NaBH_4$, dry THF, 8 h; (b) DMT-Cl, dry DCM, overnight; (c) 5 M NaOH: 1,4-dioxane, overnight; (d) NH_3, MeOH. Yield 70% for four steps (a,b,c,d). (e) and (f) NaN_3, DMF, 90 °C.

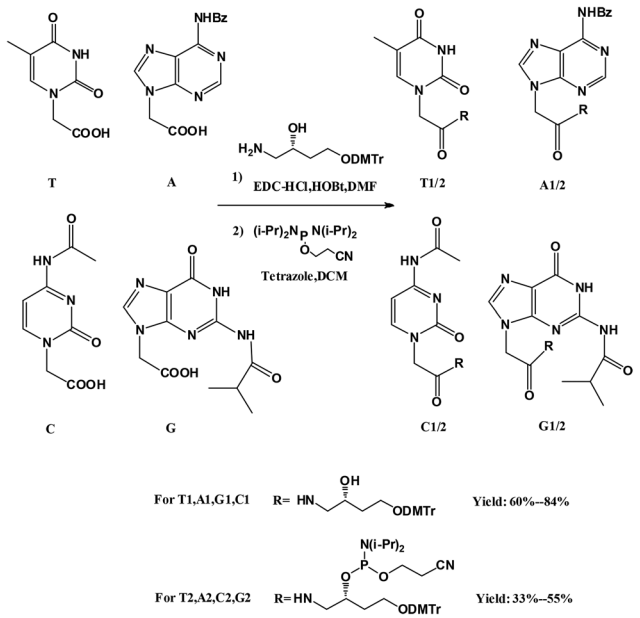

Scheme 3 Synthesis of phosphoramidite building blocks of (*R*)-Am-BuNA.

oligonucleotides are performed according to the standard protocols. After subsequent purification by RP-HPLC, the obtained oligonucleotides were characterized by ESI-MS (see Table 1).

Hybridization properties of (*R*)-Am-BuNA substituted DNA strands

In order to investigate the effect of (*R*)-Am-BuNA nucleotide substitution on ODN duplexes, we measured duplex thermal stability by UV-melting at 260 nm (see Table 2 and Fig. 1). Incorporation of one acyclic thymine or one acyclic adenine nucleotide into the middle of the sequence (see Table 2, entries 5 and 4, 6) decreased the duplex stability with ΔT_m/modification = −10 °C, −9.1 °C and −9.0 °C, respectively, compared to unmodified mmp-0/mmpsn-0 duplex. Replacement with acyclic nucleotide in the 4th- or 2nd- end of the oligonucleotide resulted in only a slight decrease in ΔT_m of −1.5 °C and −1.9 °C/modification in comparison to natural mmp-0/mmpsn-0 duplex (see Table 2, entries 3 and 7). This suggested that (*R*)-Am-BuNA modified oligonucleotides were better tolerated for the duplex formation with its complementary oligonucleotide when Am-BuNA was incorporated close to two ends of oligonucleotides due to the end-fraying phenomenon. If an acyclic cytosine instead of thymine was incorporated into the middle of mmp-0 sequence, the obtained oligonucleotide (mmp-8) can still form a duplex with the complementary sequence (mmpsn-0), but its melting temperature was 12.2 °C lower. In comparison to the duplex of mmp-5/mmpsn-0, the duplex of mmp-8/mmpsn-0 with one mismatch was less stable with lower T_m. This indicated that acyclic thymidine in mmp-5 may still have some degree of hydrogen bonding with its complementary adenine in mmpsn-0 even though the interaction of acyclic thymine/adenosine is much less stable than thymidine/adenosine of mmp-0/mmpsn-0 duplex. If all nucleotides of mmp-0 were replaced with

Table 1 Sequences of oligonucleotides used in our studies

Entry	Oligonucleotide[a]	Calculated M_w	Measured M_w
mmp-0	CACACCTTGCCATCG	4472.9	4474.0
mmp-1	**c**ACAC***c***TT***g***CC***a***TC***g***	4618.1	4619.9
mmp-2	4′-***cacaccttgccatcg***-2′	4908.4	4909.4
mmp-3	**c**ACACCTTGCCATCG	4501.9	4503.1
mmp-4	CAC**a**CCTTGCCATCG	4501.9	4502.8
mmp-5	CACACCT**t**GCCATCG	4501.9	4503.3
mmp-6	CACACCTTGCC**a**TCG	4501.9	4503.2
mmp-7	CACACCTTGCCATC***g***	4501.9	4503.1
mmp-8	CACACCT***c***GCCATCG	4486.9	4487.8
mmpsn-0	CGATGGCAAGG*T*GTG	4673.1	4675.0
mmpsn-2	4′-***cgatggcaaggtgtg***-2′	5108.5	5110.2
mmpsn-4	CGATGGCAAGG***t***GTG	4702.1	4702.6
mmpsn-5	CGATGGC***a***AGGTGTG	4702.1	4702.6
TBA-0	CGTTGGTGTGGTTGG	4726.1	4725.4
TBA-1	GGTTGG**t**GTGGTTGG	4755.1	4755.3
TBA-2	GGTT***gg***TGTGGTTGG	4784.1	4785.1
TBA-3	GG***t***TGG***t***GTGG***t***TGG	4813.1	4813.6
TBA-4	GG***tt***GGTGTGG***tt***GG	4842.1	4843.1

[a] Lower case letters represent (*R*)-Am-BuNA nucleotides and upper case letters represent DNA nucleotides.

Table 2 UV-melting studies and thermodynamic parameters (T = 310 K) of (*R*)-Am-BuNA modified duplexes and (*S*)-3-amino-1,2-propanediol nuclei acid (AmpNA) modified duplexes[c]

Entry	Duplex[a]	T_m (°C)	ΔT_m [b] (°C)	$-\Delta H$ (kJ mol^{-1})	$-\Delta S$ (J (mol K)$^{-1}$)	$-T\Delta S$ (kJ (mol K)$^{-1}$)	$\Delta G_{310\ K}$ (kJ mol^{-1})
1	mmp-0/mmpsn-0	60.0	—	293.1	878.7	272.4	−20.7
2	mmp-2/mmpsn-0	nt	—	—	—	—	—
3	mmp-3/mmpsn-0	58.5	−1.5	239.3	719.0	222.9	−16.5
4	mmp-4/mmpsn-0	50.9	−9.1	221.4	687.7	213.2	−8.2
5	mmp-5/mmpsn-0	50.0	−10.0	219.3	678.5	210.3	−9.0
6	mmp-6/mmpsn-0	51.0	−9.0	185.4	568.1	176.1	−9.3
7	mmp-7/mmpsn-0	58.1	−1.9	317.8	993.4	308.0	−9.8
8	mmp-8/mmpsn-0	47.8	−12.2	185.3	574.6	178.1	−7.2
9	AmpNA-mmp-2/mmpsn-0	nt	—	—	—	—	—
10	AmpNA-mmp-3/mmpsn-0	57.3	−2.7	214.8	653.7	202.7	−12.1
11	AmpNA-mmp-4/mmpsn-0	52.1	−7.9	208.9	642.9	199.3	−9.6
12	AmpNA-mmp-5/mmpsn-0	52.0	−8.0	200.4	613.1	190.1	−10.3
13	AmPNA-mmp-6/mmpsn-0	52.0	−8.0	214.2	654.2	202.8	−11.4
14	AmpNA-mmp-7/mmpsn-0	56.5	−3.5	284.4	892.8	276.8	−7.6

[a] See Table 1 and Table S1 for oligonucleotides sequences. [b] Decrease in melting temperature ΔT_m was calculated with respect to unmodified DNA duplex (entry 1). nt = no melting temperature was observed. Experiment conditions: 10 mM phosphate buffer, 100 mM NaCl, pH 7.2, 1 μM of each oligo strand. [c] Part of the data of AmpNA came from the published thesis of a master student from our laboratory (for comparison): Meng Su, "Functionalization and Reconstrunction of Oligonucleotides", Master thesis, Peking University, 2012.

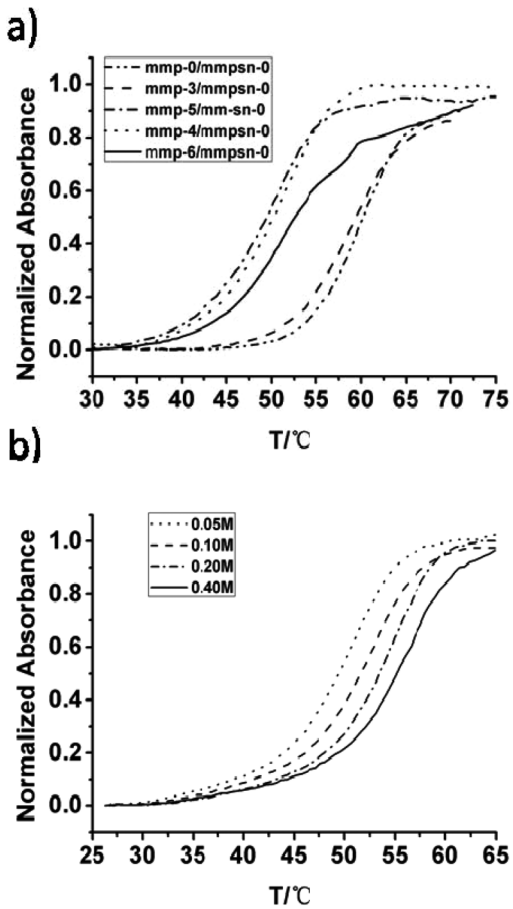

Fig. 1 (a) UV-melting profile at 260 nm of (*R*)-Am-BuNA modified DNA duplex. Experiment conditions: 1 μM for each strand of oligonucleotides in 10 mM phosphate buffer, 100 mM NaCl, pH 7.2. (b) UV-melting profile at 260 nm of mmp-5/mmpsn-0 duplex at different sodium concentrations. Experiment conditions: 1 μM for each strand of oligonucleotides in 10 mM phosphate buffer, pH 7.2 with different concentrations of NaCl.

acyclic nucleotides, no T_m was observed for the duplex of the obtained oligonucleotide (mmp-2) and mmpsn-0, which is normal for most of the nucleic acids modified with acyclic nucleotide analogues, such as (*S*)-BuNA,[17] UNA[7] or TNA[14a] under similar salt conditions. By shortening the distance of three carbons to two carbons between two backbone phosphates, we obtained another artificial nucleic acid analogues, (*S*)-AmpNA) with (*S*)-3-amino-1,2-propanediol as scaffold which was previously synthesized in our lab. These artificial nucleic acid analogues did not show much better improvement on the thermodynamic stability on duplex formation (see Table 2 and ESI S2†). Incorporation of one AmpNA nucleotide into the end of the oligonucleotide (Table 2, entries 10 and 14) leads to decrease in T_m of about −3 °C/modification. When we incorporated AmpNA nucleotides in the middle of the sequences (Table 2, entries 11–13), a sharp decrease of ΔT_m values was observed. These unstable duplexes between acyclic nucleotide modified oligonucleotide and its complementary natural DNA was thought to be the flexible backbone. For oligonucleotide analogues containing all (*R*)-Am-BuNA and (*S*)-AmpNA monomers, no better hybridization property was found in comparison to natural DNA, probably due to the fact that there is a more flexible linkage between the nucleobase and backbone, in addition to the flexible backbone as others. The flexibility of the acyclic nucleotide might cause an unfavorably large loss in entropy upon duplex formation. Thermodynamic parameters in the process of duplex formation (see Table 2) were then evaluated using the van't Hoff plot. Under a two-state transition model, K_a, the equilibrium constant, refers to the folding and unfolding of the duplex. Assuming that enthalpy and entropy are independent of temperature and Gibbs equation $\Delta G = -RT\ln(K_a) = \Delta H - T\Delta S$, the plot of $\ln(K_a)$ against $1/T$ (K^{-1}) gave a straight line with $r^2 >$ 0.99 (ESI S4†). The slope and intercept of the straight line corresponded to $(-\Delta H/R)$ and $(\Delta S/R)$, respectively, as shown in Table 2. As expected, the lower thermal stabilities of the acyclic

nucleotide modification duplex correlated with lower thermodynamic parameters (310 K) except for the 2′-end modified duplex mmp-7/mmpsn-0. The $-T\Delta S$ value of mmp-7/mmpsn-0 exceeded that of mmp-0/mmpsn-0, indicating that a 2′-end guanine modified duplex showed higher enthalpy and entropy than natural DNA, which is quite different from other acyclic nucleotide modified duplexes in Table 2. This observation is similar to a previous study with GNA, in which acyclic nucleotide modification duplex formation is less exothermic than DNA duplex formation, but at the same time entropically significantly less unfavorable due to a stacking interaction of acyclic modification at the 2′-end.[9] The free energy (ΔG) of the duplexes at 310 K was also calculated as listed in Table 2, which suggested that all (*R*)-Am-BuNA modified duplexes could be formed under physiological pH and salt concentrations. The values of ΔG correlated with the T_m of the corresponding duplexes. Furthermore, considering the effect of salt bridge on the nucleic acid duplex, we investigated the effect of Na^+ concentration on the T_m value. The duplex of mmp-5/mmpsn-0 was significantly stabilized with increasing NaCl concentration from 0.05, 0.10, and 0.20 to 0.40 M, respectively, as shown in Fig. 1b.

Fig. 2 shows the melting curves of the duplexes of (*R*)-Am-BuNA, double-stranded ODNs with two complementary acyclic nucleotide modifications and double-stranded natural ODNs. The thermal stability of the (*R*)-Am-BuNA duplex mmp-2/mmpsn-2 (T_m = 41.2 °C) was significantly lower than one acyclic nucleotide modification duplex (T_m = 51.2 °C) and DNA duplex (T_m = 60.0 °C) with the decrease of T_m by 8.8 °C and 18.8 °C, respectively. This observation of lower stability of pure duplex of (*R*)-Am-BuNA is different from previous reports of GNA, TNA or SNA, but similar to (*S*)-BuNA. We further investigated the effect of salt concentration on the stability of acyclic nucleotide modified oligonucleotide duplex, however, no apparent differences were observed with the increase in salt concentrations from 0.05 M to 0.20 M. Slight increase of T_m (~1.0 °C) under a strong electrolyte condition (salt concentration, 0.40 M) was observed. The results showed a weak connection between salt concentrations and T_m values in comparison to that of one acyclic nucleotide modified oligonucleotide duplex. A possible reason for the inefficient reorganization of oligonucleotide duplexes with acyclic nucleotide modification may be ascribed to the longer and more flexible linkage between the base and backbone than that of natural DNA, leading to an unstable duplex and a lower contribution of ionic bond between negative charge in the backbone and positive charge ions to the stabilization of duplex in physiological environments.

CD experiments were carried out to elucidate the duplex conformation of mmp-2/mmpsn-2 as well as natural ODNs. As shown in Fig. 3, the CD spectrum of mmpsn-2 alone was associated with weak cotton effect and showed weak broad positive peak at 230–260 nm, which indicated that no preorganized structure was formed. Further investigation of the mmp-2/mmpsn-2 duplex showed that its CD spectrum contained strong positive peaks at 280 nm and 240 nm and a negative peak at 260 nm with a crossover at 257 nm. This observation clearly indicated duplex formation between these two strands.

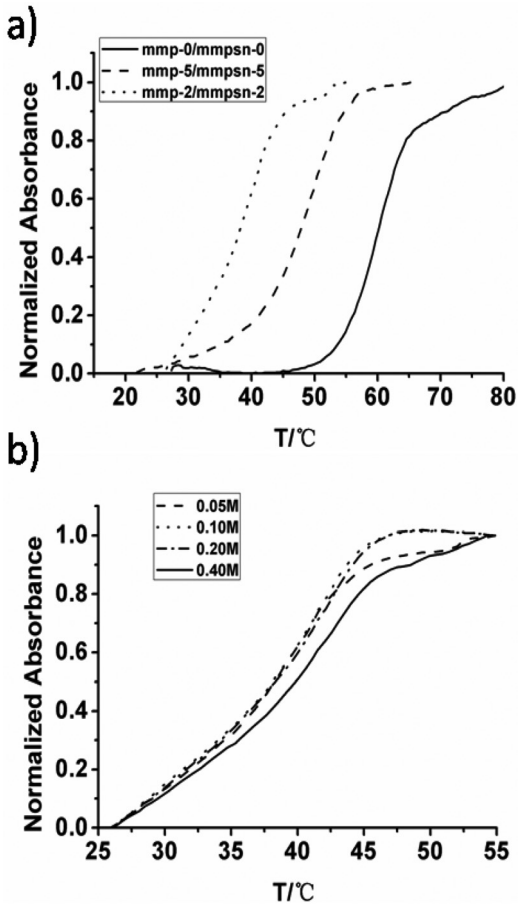

Fig. 2 (a) UV-melting profile at 260 nm of (*R*)-AM-BuNA duplex. Experiment conditions: 1 μM for each strand of oligonucleotides in 10 mM phosphate buffer, 100 mM NaCl, pH 7.2. (b) UV-melting profile at 260 nm of mmp-2/mmpsn-2 duplex at different sodium concentrations. Experiment conditions: 1 μM for each strand of oligonucleotides in 10 mM phosphate buffer, pH 7.2 with different concentrations of NaCl.

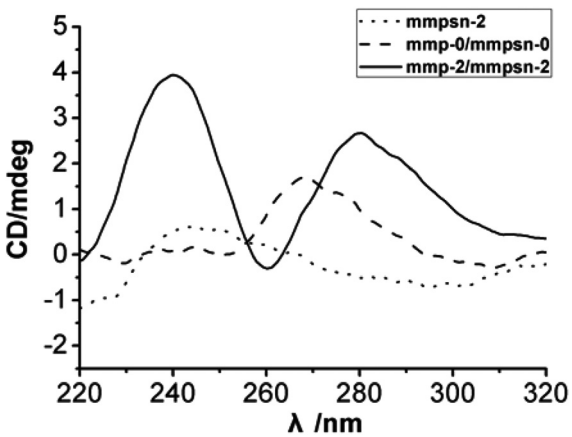

Fig. 3 CD profiles of natural and acyclic nucleotide-modified oligonucleotide duplexes. Experiment conditions: 5 μM for each strand of oligonucleotides in 10 mM phosphate buffer, 100 mM NaCl, pH 7.2, at 25 °C.

Table 3 UV-melting studies and thermodynamic parameters of (*R*)-Am-BuNA modified TBA (T = 310 K)

Entry	Duplex[a]	T_m (°C)	ΔT_m [b] (°C)	$-\Delta H$ (kJ mol^{-1})	$-\Delta S$ (J (mol K)$^{-1}$)	$-T\Delta S$ (kJ (mol K)$^{-1}$)	$\Delta G_{310\ K}$ (kJ mol^{-1})
1	TBA-0	49.8	—	178.3	554.2	171.8	−6.6
2	TBA-1	50.8	1.0	162.2	501.1	155.3	−6.8
3	TBA-2	36.0	−13.8	111.4	353.5	109.6	−1.9
4	TBA-3	nt	nt	—	—	—	—
5	TBA-4	39.6	−10.2	149.7	480.6	149.0	−0.7

[a] See Table 1 for oligonucleotides sequences. [b] Decrease in melting temperature ΔT_m was calculated with respect to unmodified TBA oligonucleotide (entry 1). nt = no melting temperature was observed. Experiment conditions: 5 μM oligonucleotides in 10 mM Tris-HCl buffer, 100 mM KCl, pH 7.4.

In addition, the positive peak at 280 nm and a crossover at 257 nm of the acyclic nucleotide modified nucleic acid duplex were in accordance with the characteristics of right-handed nucleic acids.

Quadruplex formation of (*R*)-Am-BuNA modified TBA aptamers

According to previous NMR and X-ray structural studies, TBA forms an intramolecular antiparallel G-quadruplex with two G-tetrads linked by three loops: a central TGT and two TT loops.[18] Further studies on the properties of modified TBA shows that modifications with acyclic nucleotide monomers at 3rd, 7th and 12th positions of this sequence resulted in an increased thermal stability, especially at the 7th position.[19] Thus, we synthesized two TBA oligonucleotides by incorporation of one acyclic monomer at the 7th position (TBA-1) and three acyclic monomers at 3rd, 7th and 12th positions (TBA-3). Modifications with acyclic (*R*)-Am-BuNA monomers at G-tetrads (TBA-2) and two TT loops (3rd and 4th, 12th and 13th positions, TBA-4) were also achieved to investigate their thermal stability. The results of UV melting studies at 295 nm are shown in Table 3 and Fig. 4a. It is clearly seen that modification at the 7th position slightly increased the thermal stability with the ΔT_m value of 1.0 °C compared to that of natural TBA-0. Unexpectedly, for TBA-3 with three acyclic nucleotide modifications at the 3rd, 7th and 12th positions, no T_m was observed. Acyclic nucleotide modification in the region of G-tetrads and two TT loops also lowered the thermal stability of modified aptamers with ΔT_m values of −13.8 °C and −10.2 °C, respectively. These results suggested that incorporation of (*R*)-Am-BuNA monomer only at the 7th position in the TBA sequence was favorable for quadruplex formation. Next, the effect of potassium concentration on quadruplex formation was also investigated. The 7th modified quadruplex TBA-1 was treated with different concentrations of potassium ion (0.01 M, 0.05 M, 0.10 M, 0.20 M and 0.40 M). As we expected, gradual increase of T_m values was observed with the increase of potassium concentrations, as shown in Fig. 4b.

Melting curves of each modified TBA quadruplex provided the thermodynamic parameters as shown in Table 3. Modification at G-tetrads (TBA-2) resulted in the destabilization of the quadruplex structure due to a sharp decrease of ΔH. This suggested that acyclic modification in the G-tetrads region was unfavorable for quadruplex formation. Thermodynamics

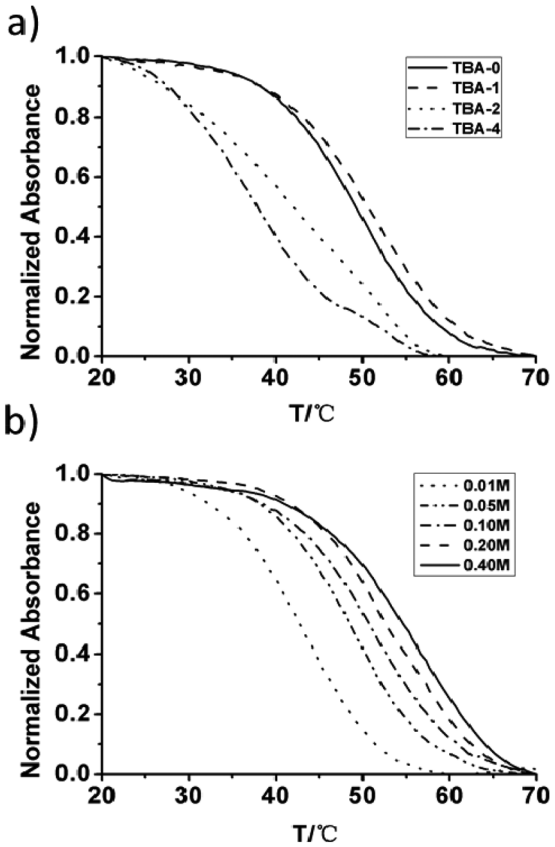

Fig. 4 (a) UV-melting profile at 295 nm of (*R*)-Am-BuNA modified TBA. Experiment conditions: 10 mM Tris-HCl buffer, 100 mM KCl, pH 7.4, 5 μM oligonucleotide strand concentration. (b) UV-melting profile at 295 nm of TBA-2 at different potassium concentrations. Experiment conditions: 10 mM Tris-HCl buffer, pH 7.4, 5 μM oligo strand concentration with different concentrations of KCl.

parameters of the 7th modified G-quadruplex (TBA-1) shows a favorable ΔG compared to that of natural TBA-0. However, incorporation of multiple acyclic thymines (TBA-3) caused a disadvantageous effect, which indicated that more flexible structures might restrict the spatial folding process of the G-quadruplex. CD spectra were further recorded for natural TBA and (*R*)-Am-BuNA modified TBAs (Fig. 5). It is clearly seen that positive peaks at 250 nm and 290 nm and a negative peak at 270 nm were observed in the CD spectrum of the 7th position modified quadruplex (TBA-1) which is in accordance with

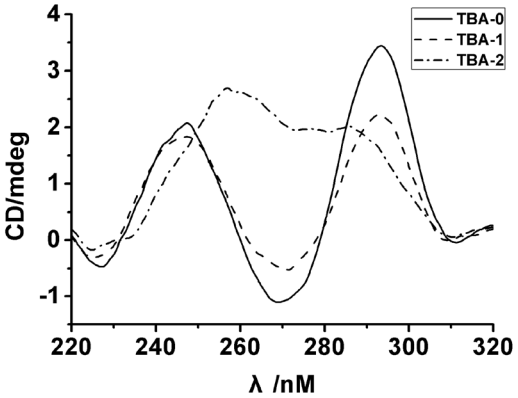

Fig. 5 CD profile of natural TBA and (*R*)-Am-BuNA modified TBAs. Experiment conditions: 1 μM for each strand of oligonucleotides in 10 mM Tris-HCl buffer, 100 mM KCl, pH 7.4, at 25 °C.

that of natural TBA-0. This suggested that acyclic modification at the 7th position did not cause any disadvantageous effect on the formation of antiparallel G-quadruplex. TBA-2 with acyclic monomer incorporation into G-tetrads showed a broad positive CD spectrum between 230 and 310 nm that is completely different from that of the antiparallel G-quadruplex of the natural TBA. The complicated CD spectra may be due to multiple conformations of TBA-2, which was consistent with the observation of unclear transition in the T_m melting curve. Incorporation of multiple acyclic nucleobases (TBA-4) further caused the loss of CD signals due to non-organized conformations.

Enzymatic stability of (*R*)-Am-BuNA modified ODNs

Together with the natural sequences of mmp-0 and TBA-0, (*R*)-Am-BuNA modified ODNs (mmp-7 and TBA-1) were treated with fetal bovine serum (FBS) and snake venom phosphodiesterase (SVPDE), respectively. All oligonucleotides species were individually incubated in FBS and SVPDE, and aliquots were then sampled at regular intervals, quickly frozen and stored for gel-shift analysis. (Fig. 6). When incubated in 20% FBS at 37 °C, mmp-0 was almost completely degraded in 480 min, while mmp-7 with single terminal (*R*)-Am-BuNA modification showed little degradation even after 960 min incubation, as shown in Fig. 6a. If SVPDE was used, mmp-0 degraded very fast and almost disappeared in 20 min. Instead, only a small amount of degradation of mmp-7 was observed in 60 min incubation at the same concentration of SVPDE (Fig. 6c). Similar to mmp-7, we observed the increased enzymatic stability of (*R*)-Am-BuNA modified TBA-1 than that of TBA-0, as shown in Fig. 6b and 6d. These results indicated that single modification of oligonucleotides with (*R*)-Am-BuNA could greatly enhance their resistance to enzymatic degradation. This is because the artificial nucleotide is not recognized by some *exo*-nucleases, which is similar to a previously reported glycerol derived building block as terminal modification.[9]

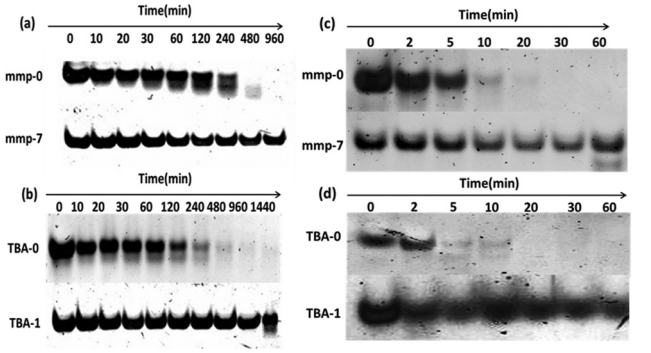

Fig. 6 (a) Stability of unmodified and acyclic nucleotide-modified single oligonucleotide strand in FBS. Experiment conditions: 10 μM mmp-0 or mmp-7 in 20% FBS at 37 °C. (b) Stability of unmodified (TBA-0) and acyclic nucleotide-modified anti-thrombin-binding aptamer (TBA-1) in FBS. Experiment conditions: 10 μM TBA-0 or TBA-1 in 40% FBS at 37 °C. (c) Stability of unmodified and acyclic nucleotide-modified single oligonucleotide strand in SVPDE. Experiment conditions: 5 μM mmp-0 or mmp-7 with 220 mU SVPDE in 100 mM Tris-HCl buffer, 10 mM $MgCl_2$, 100 mM NaCl, pH 7.4, at 37 °C. (d) Stability of unmodified and acyclic nucleotide-modified thrombin-binding DNA aptamer in SVPDE. Experiment conditions: 5 μM TBA-0 or TBA-1 with 330 mU SVPDE in 100 mM Tris-HCl buffer, 10 mM $MgCl_2$, 100 mM KCl, pH 7.4, at 37 °C.

Conclusions

Artificial nucleic acid analogues, (*R*)-Am-BuNA with a (*R*)-4-aminobutane-1,3-diol backbone, were synthesized and their thermal stability of duplexes and G-quadruplexes was demonstrated. Similar to other acyclic nucleotide analogues, incorporation of acyclic (*R*)-4-aminobutane-1,3-diol scaffold at different positions in DNA strands induced a decreased thermal stability. A significantly less effect on the decrease of T_m was experienced with acyclic nucleotide modifications close to the two terminals, and modifications in the middle of the sequences resulted in a marked decrease in the T_m value. Increasing the backbone length by one carbon atom resulted in no significant difference of duplex thermal stability of nucleic acid analogues with (*R*)-4-amino-butane-1,3-diol in comparison to (*S*)-3-amino-1,2-propanediol as scaffolds. It seems that the long linkage of an amide bond in the side chain shows no favorable effect on the formation of duplex in comparison to that of (*S*)-BuNA due to the flexible backbone and flexible linkage of the backbone and nucleobases. The data of acyclic (*R*)-Am-BuNA modified TBAs indicated that modification at the 7′ position of the TBA sequence resulted in comparable thermal stability and maintained the same conformation of anti-parallel G-quadruplex as that of the natural TBA. Multiple modifications of TBA sequences at the loop and G-tetrads are unfavorable. Further enzymatic experiments revealed that oligonucleotides with even single acyclic (*R*)-Am-BuNA modification greatly enhanced their enzymatic stability. These studies indicated that the extended distances between the backbone units or the backbone and nucleobase caused an unfavorable effect on the duplex thermodynamic stability,

providing additional information on DNA base pairing. The enzymatic stability of oligonucleotides with single modification of (*R*)-Am-BuNA analogues shows their possible applications as capping nucleobases for high stable nucleic acids drugs.

Experimental section

Synthesis of acyclic (*R*)-Am-BuNA monomers

(3*R*)-4-Chloro-1,3-butanediol (B1). Sodium borohydride (0.68 g, 18.0 mmol) was dissolved in THF (10 mL). The mixture was warmed at 40 °C for 30 min. To this mixture was added dropwise ethyl-(3*R*)-4-chloro-3-hydroxyl butyrate (98% ee, 2.15 g, 12.9 mmol, Beijing Ouhechem Technology Co. Ltd). The reaction continued for another 5 hours and was then quenched with hydrochloric acid (2 mL concentrated HCl in 5 mL water) at 0 °C. The mixture was stirred for one more hour and was then adjusted to pH = 7 with aqueous sodium hydroxide. The solution was extracted with ethyl acetate (50 mL) and the organic layer was combined and dried with anhydrous Na_2SO_4. After filtration, the organic solvent was removed *in vacuo* and the crude residue was purified by flash column chromatography (PE–EA, 1/10) to afford the compound **B1** (1.55 g, 12.4 mmol) as a pale-yellow oil with 96% yield. $[\alpha]_D^{25}$ = 22.3 (*c* = 1.09, methanol); ^{1}H-NMR (400 MHz, $CDCl_3$) δ = 3.99–4.05 (m, 1 H), 3.82 (m, *J* = 10.4, 9.0, 3.9 Hz, 2 H), 3.59 (dd, *J* = 11.1, 4.3 Hz, 1H), 3.50 (dd, *J* = 11.1, 6.6 Hz, 2 H), 1.72–1.78 (m, 1 H). ^{13}C-NMR (100 MHz, $CDCl_3$) δ = 70.8, 60.4, 49.7, 35.7.

(3*R*)-4-Chloro-1-(bis(4-methoxyphenyl)(phenyl)methoxy)-3-butanol (B2). **B1** (400 mg, 3.2 mmol) and DMT-Cl (1.08 g, 3.2 mmol) were dissolved in dichloromethane (15 mL). Under N_2, 1 mL of triethylamine was added dropwise carefully at 0 °C. The mixture was stirred overnight, and then diluted with dichloromethane (50 mL). The obtained solution was washed with saturated sodium bicarbonate solution (20 mL × 3). The organic layer was combined and dried with anhydrous Na_2SO_4. After filtration, the organic solvent was removed *in vacuo* to afford the compound **B2** (1.23 g, 2.88 mmol) as a pale-yellow oil with a yield of 90%. R_f value was given 0.5 in PE–EA 3/1. ^{1}H-NMR (400 MHz, $CDCl_3$) δ = 7.38 (d, *J* = 7.3 Hz, 2H), 7.24–7.29 (m, 7 H), 6.80 (d, *J* = 8.8 Hz, 4 H), 3.97–4.00 (m, 1 H), 3.75 (s, 6 H), 3.43–3.52 (m, 2 H), 3.34 (dd, *J* = 5.4, 4.3 Hz, 1H), 3.25 (dd, *J* = 5.5, 4.0 Hz, 1 H), 1.79–1.82 (m, 2 H); ^{13}C-NMR (100 MHz, $CDCl_3$) δ = 158.6, 144.8, 136.0, 135.9, 128.1, 128.0, 127.0, 113.2, 86.8, 70.8, 61.3, 55.3, 49.5, 34.0.

(3*R*)-1-(Bis(4-methoxyphenyl)(phenyl)methoxy)-3,4-epoxybutane (B3). To a solution of **B2** (450 mg, 1.1 mmol) in 1,4-dioxane (5 mL), 5 M sodium hydroxide solution was added dropwise. The solution was stirred overnight at 40 °C and was then diluted with ethyl acetate (50 mL). The mixture was washed with saturated sodium chloride solution (10 mL × 3). The organic layer was combined and dried with anhydrous Na_2SO_4. After filtration, the organic solvent was removed *in vacuo* to afford pale-yellow oil **B3** (420 mg, 1.1 mmol) with a yield of 98%. R_f value was given 0.3 in PE–EA (10/3). $[\alpha]_D^{25}$ = 6.7 (*c* = 1.16, methanol); ^{1}H-NMR (400 MHz, $CDCl_3$) δ = 7.44 (d, *J* = 7.6 Hz, 2 H), 7.16–7.34 (m, 7 H), 6.83 (d, *J* = 8.8 Hz, 4 H), 3.75 (s, 6 H), 3.20–3.26 (m, 2 H), 3.09–3.12 (m, 1 H), 2.80 (dd, *J* = 8.2, 5.0 Hz, 1 H), 2.51 (dd, *J* = 5.0, 2.7 Hz, 1 H), 1.79–1.83 (m, 2 H); ^{13}C-NMR (100 MHz, $CDCl_3$) δ = 158.2, 144.9, 136.2, 129.9, 129.0, 127.6, 126.6, 113.0, 85.9, 60.3, 55.1, 50.3, 47.1, 33.2; *m*/*z* MS (ESI-TOF$^+$) measured $[M + Na]^+$ 413.32, $C_{25}H_{26}O_4$, calculated $[M + Na]^+$ 413.18.

(3)-4-Amino-1-(bis(4-methoxyphenyl)(phenyl)methoxy)-3-butanol (B4). The product **B3** (0.32 g, 0.82 mmol) was dissolved in a saturated solution of ammonium in methanol. The mixture was stirred for 24 h and then concentrated *in vacuo*. The crude residue was purified by flash chromatography (DCM–MeOH–TEA, 10/1/1%) to afford **B4** (245 mg, 0.60 mmol) as a colorless viscous oil with a yield of 75%; $[\alpha]_D^{25}$ = 2.3 (*c* = 1.06, methanol); ^{1}H-NMR (400 MHz, $CDCl_3$) δ = 7.43(d, *J* = 7.4 Hz, 2 H), 7.18–7.32 (m, 7 H), 6.83 (d, *J* = 8.8 Hz, 4 H), 3.78 (s, 6 H), 3.72 (m, 1 H), 3.30 (m, 1 H), 3.22 (m, 1 H), 2.75 (dd, *J* = 12.6, 3.5 Hz, 1 H), 2.58 (dd, *J* = 12.7, 7.8 Hz, 1 H), 1.67–1.77 (m, 2 H); ^{13}C-NMR (100 MHz, $CDCl_3$) δ = 158.5, 145.0, 136.2, 136.1, 130.0, 128.1, 127.9, 126.8, 113.2, 86.6, 71.6, 61.8, 55.3, 47.7, 34.5; *m*/*z*: MS (ESI-TOF$^+$) measured $[2M + H]^+$ 815.4250, $C_{25}H_{29}NO_4$, calculated $[2M + H]^+$ 815.4266.

General method for coupling of acetic-bases and acyclic backbone (B4)

Acyclic backbone **B4** (1.0 eq.), acetic-base (**A**, **G**, **C**, **T**, 1.1 eq.), EDC-HCl (1.5 eq.), HOBt (1.5 eq.), and TEA (3.0 eq.) were suspended in anhydrous DMF (0.5 mmol mL^{-1}). After stirring for 1 hour at room temperature, chloromethane was added to dilute the mixture. The solution was washed with brine three times and the organic layer was combined and concentrated. Cold ether was added to the residue and the mixture was left at −4 °C overnight. The desired building blocks (**A1**, **G1**, **C1** and **T1**) were obtained by filtration and used for the following steps without further purification.

A1 for adenine (A1). White solid (67% yield), $[\alpha]_D^{25}$ = −5.6 (*c* = 1.03, methanol) ^{1}H-NMR: (400 MHz, $CDCl_3$) δ = 8.65 (s, 1 H), 8.09 (s, 1 H), 7.98 (d, *J* = 7.6 Hz, 2 H), 7.58 (d, *J* = 7.1 Hz, 1 H), 6.80–7.55 (m, 11 H), 6.80 (d, *J* = 8.4 Hz, 4 H), 4.90 (s, 2 H), 3.94 (s, 1 H), 3.76 (2, 1 H) 3.52–3.76 (m, 1 H), 3.24 (m, 1 H), 3.13–3.18 (m, 2 H), 1.71–1.76 (m, 2H); ^{13}C-NMR (100 MHz, $CDCl_3$) δ = 166.0, 165.0, 158.4, 152.5, 152.0, 149.3, 144.7, 143.8, 135.9, 135.8, 133.5, 132.7, 129.9, 128.7, 128.0, 127.9, 126.8, 122.4, 113.2, 86.7, 69.4, 61.4, 55.2, 46.3, 45.8, 34.4; *m*/*z* MS (ESI-TOF$^+$) measured $[M + Na]^+$ 709.58, $C_{39}H_{38}N_6O_6$ calculated $[M + Na]^+$ 709.28.

G1 for guanine (G1). White solid (59% yield), $[\alpha]_D^{25}$ = −2.3 (*c* = 0.97, methanol) ^{1}H-NMR (400 MHz, DMSO-d_6): 8.21 (s, 1 H), 7.90 (s, 1 H), 7.36 (d, *J* = 7.8 Hz, 2 H), 7.30 (d, *J* = 7.6 Hz, 2 H), 7.22–7.35 (m, 5 H), 6.87 (d, *J* = 8.6 Hz, 4 H), 5.75 (s, 1 H), 4.79 (s, 2 H), 4.65–4.66 (d, *J* = 5.4 Hz, 2 H), 3.73 (s, 6 H), 3.67 (br, 1 H), 3.20–3.32 (m, 1 H), 3.03 (m, 3 H), 2.50–2.78 (m, 2 H), 1.51–1.72 (m, 2 H), 1.09 (d, *J* = 6.7 Hz, 6 H); ^{13}C-NMR (100 MHz, DMSO-d_6) δ = 180.1, 166.1, 157.9, 154.9, 149.0, 147.9, 145.2, 140.8, 129.6, 127.7, 127.6, 126.5, 119.7, 113.1,

85.3, 66.4, 60.2, 55.0, 45.6, 45.3, 34.9, 34.7, 18.9. *m*/*z* MS (ESI-TOF$^+$) measured $[M + Na]^+$ 691.58, $C_{36}H_{40}N_6O_7$ calculated $[M + Na]^+$ 691.73.

C1 for cytosine (C1). White solid (84.4% yield), $[\alpha]_D^{25} = -8.7$ (*c* = 0.98, methanol); ^{1}H-NMR (400 MHz, $CDCl_3$) δ = 9.38 (s, 1 H), 7.56–7.63 (m, 1 H), 7.53–7.55 (m, 1 H), 7.40–7.52 (m, 3 H), 7.28–7.50 (m, 10 H), 6.81 (d, *J* = 8.9 Hz, 4 H), 4.46–4.60 (m, 2 H), 3.96 (m, 1H), 3.78 (s, 7 H), 3.44–3.55 (m, 1 H), 3.24–3.37 (m, 1 H), 3.20 (m, 1 H), 3.07 (m, *J* = 13.3, 8.1, 5.4 Hz, 1 H), 2.15 (s, 3 H), 1.71 (m, 2 H); ^{13}C-NMR (100 MHz, $CDCl_3$) δ = 170.8, 166.7, 162.6, 157.9, 155.2, 151.4, 145.2, 136.0, 129.6, 127.7, 127.6, 126.5, 113.1, 94.6, 85.2, 66.4, 60.1, 55.0, 51.4, 45.7, 45.5 (triethylamine), 34.8, 24.3, 11.6 (triethylamine); *m*/*z* MS (ESI-TOF$^+$) measured $[M + Na]^+$ 623.13, calculated $C_{33}H_{36}N_4O_7$ $[M + Na]^+$ 623.66.

T1 for thymine (T1). White solid (75% yield), $[\alpha]_D^{25} = -4.4$ (*c* = 1.00, methanol), ^{1}H-NMR (400 MHz, $CDCl_3$), δ = 7.40–7.41 (m, 1 H), 7.38 (s, 1 H), 7.27–7.30 (m, 6 H), 7.21 (m, *J* = 7.2 Hz, 1H), 7.04–7.18 (m, 1H), 6.82 (m, *J* = 8.9 Hz, 2 H), 4.27 (s, 1 H), 3.92 (m, 1H), 3.79 (s, 6 H), 3.44–3.49 (m, 1 H), 3.32–3.40 (m, 1 H), 3.20–3.27 (m, 1 H), 3.04–3.17 (m, 1 H), 1.88 (s, 3 H), 1.69–1.77 (m, 2 H); ^{13}C-NMR (100 MHz, $CDCl_3$) δ = 167.00, 164.5, 158.6, 151.4, 144.8, 140.9, 136.0, 130.0, 128.1, 128.0, 127.0, 113.3, 111.1, 86.9, 69.9, 61.8, 55.3, 50.55, 46.2, 45.6 (triethylamine), 36.6 (DMF), 34.4, 12.4. *m*/*z* MS (ESI-TOF$^+$) measured $[M + Na]^+$ 596.32, $C_{32}H_{35}N_3O_7$ calculated $[M + Na]^+$ 596.24.

General method for phosphoramidition

Dry DMT protected nucleotides (**A1**, **G1**, **C1**, **T1**, 1.0 eq.) and 1-H-tetrazole were dissolved in anhydrous dichloromethane (200 mg/2 mL) under N_2 conditions. 2-Cyanoethyl *N*,*N*,*N*′,*N*′-tetraisopropylphosphorodiamidite (4.0 eq.) was dissolved in anhydrous dichloromethane (2 mL) and was added to the reaction system. The mixture was stirred at room temperature for 2 h, the corresponding (*R*)-Am-BuNA monomers (**A2**, **G2**, **C2**, **T2**) were then purified through flash silica gel column chromatography.

A2. Eluent solution: dichloromethane–TEA, 100/2. 54% yield, ^{1}H-NMR (400 MHz, $CDCl_3$) δ = 8.79 (s, 1 H), 8.20 (s, 1 H), 8.15 (s, 2 H), 7.29–7.61 (m, 12 H), 6.82 (d, *J* = 8.5 Hz, 4 H), 4.90–4.97 (m, 2 H), 4.13 (m, 1 H), 3.18–3.76 (m, 14 H), 2.69–2.71 (m, 1 H), 2.46–2.49 (m, 1 H), 1.83–1.87 (m, 2 H), 1.00–1.13 (m, 12 H). ^{31}P-NMR (162 MHz, $CDCl_3$) δ = 146.5, 148.1. *m*/*z* MS (ESI-TOF$^+$) measured $[M + Na]^+$ 910.29, $C_{48}H_{55}N_8O_7P$ calculated $[M + Na]^+$ 909.97.

G2. Eluent solution: dichloromethane–acetone–TEA, 100/10/2. 54% yield, ^{1}H-NMR (400 MHz, $CDCl_3$) δ = 7.70 (d, 1 H, *J* = 12.6 Hz), 7.37–7.39 (m, 2 H), 7.19–7.22 (m, 8 H), 6.81 (m, 4 H), 4.70 (m, 2 H), 4.12 (m, 1 H), 3.78 (s, 6 H), 3.12–3.78 (m, 8 H), 2.63 (s, 2 H), 1.78–1.88 (m, 3 H), 1.01–1.19 (m, 12 H). ^{31}P-NMR (162 MHz, $CDCl_3$) δ = 146.2, 148.2. *m*/*z* MS (ESI-TOF$^+$) measured $[M + Na]^+$ 892.22, $C_{45}H_{75}N_8O_8P$ calculated $[M + Na]^+$ 891.96.

C2. Eluent solution: dichloromethane–TEA, 100/3. 33% yield, ^{1}H-NMR (400 MHz, $CDCl_3$) δ = 7.71 (d, *J* = 7.3 Hz, 1 H), 7.28–7.43 (m, 9 H), 7.20 (m, 1 H), 6.81–6.84 (m, *J* = 4.2, 8.4 Hz, 4H), 4.50 (m, 2 H), 4.12 (m, 1 H), 3.78 (s, 6 H), 3.12–3.78 (m, 8 H), 2.23 (s, 3 H), 1.82–1.99 (m, 4 H), 1.01–1.16 (m, 12 H). ^{31}P-NMR (162 MHz, $CDCl_3$) δ = 146.8, 148.1. *m*/*z* MS (ESI-TOF$^+$) measured $[M + Na]^+$ 824.29, $C_{42}H_{53}N_6O_8P$ calculated $[M + Na]^+$ 823.88.

T2. Eluent solution: dichloromethane–TEA, 100/2, 51% yield; ^{1}H-NMR (400 MHz, $CDCl_3$) δ = 7.15–7.32 (m, 9 H), 7.10 (s, 1 H), 7.05 (s, 1 H), 6.85 (t, *J* = 4.8, 8.8 Hz, 4 H), 4.36 (m, 2 H), 3.89 (m, 1 H), 3.80 (s, 6 H), 3.16–3.78 (m, 8 H), 2.51 (m, 1 H), 2.17 (m, 1 H), 1.84–1.92 (m, 5 H), 1.03–1.17 (m, 12 H); ^{31}P-NMR (162 MHz, $CDCl_3$) δ = 146.6, 148.0. *m*/*z* MS (ESI-TOF$^+$) measured $[M + Na]^+$ 797.14, $C_{41}H_{52}N_5O_8P$ calculated $[M + Na]^+$ 796.85.

Acknowledgements

This work was supported by the National Basic Research Program of China (973 Program; grant no. 2012CB720600), the National Natural Science Foundation of China (grant no. 21072015), Program for New Century Excellent Talents in University (grant no. NCET-10-0203) and the State Key Laboratory of Drug Research (grant no. SIMM1106KF-15).

Notes and references

1 (*a*) A. Ray and B. Nordén, *FASEB J.*, 2000, **14**, 1041–1060; (*b*) N. Dias and C. A. Stein, *Mol. Cancer. Ther.*, 2002, **1**, 347–355; (*c*) J. Heasman, *Dev. Biol.*, 2002, **243**, 209–214; (*d*) S. Shukla, C. S. Sumaria and P. I. Pradeepkumar, *ChemMedChem*, 2010, **5**, 328–349; (*e*) J. K. Watts and D. R. Corey, *J. Pathol.*, 2012, **226**, 365–379; (*f*) J. Fu, M. Liu, Y. Liu and H. Yan, *Acc. Chem. Res.*, 2012, **45**, 1215–1226; (*g*) E. L. Chernolovskaya and M. A. Zenkova, *Curr. Opin. Mol. Ther.*, 2010, **12**, 158–167; (*h*) N. C. Seeman and P. S. Lukeman, *Rep. Prog. Phys.*, 2005, **68**, 237–270.

2 (*a*) F. Reck, H. Wippo, R. Kudick, M. Bolli, G. Ceulemans, R. Krishnamurthy and A. Eschenmoser, *Org. Lett.*, 1999, **1**, 1531–1534; (*b*) K. U. Schoning, P. Scholz, S. Guntha, X. Wu, R. Krishnamurthy and A. Eschenmoser, *Science*, 2000, **290**, 1347; (*c*) V. B. Pinheiro and P. Holliger, *Curr. Opin. Chem. Biol.*, 2012, **16**, 245–252; (*d*) V. B. Pinheiro, A. I. Taylor, C. Cozens, M. Abramov, M. Renders, S. Zhang, J. C. Chaput, J. Wengel, S.-Y. Peak-Chew and S. H. McLaughlin, *Science*, 2012, **336**, 341–344; (*e*) M. Stoop, G. Meher, P. Karri and R. Krishnamurthy, *Chemistry*, 2013, **19**, 15336–15345.

3 P. E. Nielsen, M. Egholm, R. H. Berg and O. Buchardt, *Science*, 1991, **254**, 1497–1500.

4 M. Egholm, O. Buchardt, L. Christensen, C. Behrens, S. M. Freier, D. A. Driver, R. H. Berg, S. K. Kim, B. Norden and P. E. Nielsen, *Nature*, 1993, **365**, 566–568.

5 (*a*) P. E. Nielsen, *Chem. Biol.*, 2010, **7**, 786–804; (*b*) E. Rozners, *J. Nucleic Acids*, 2012, **2012**, 518162.

6 (*a*) M. A. Campbell and J. Wengel, *Chem. Soc. Rev.*, 2011, **40**, 5680–5689; (*b*) N. Langkjær, A. Pasternak and

J. Wengel, *Bioorg. Med. Chem.*, 2009, **17**, 5420–5425; (*c*) M. M. Mangos, K.-L. Min, E. Viazovkina, A. Galarneau, M. I. Elzagheid, M. A. Parniak and M. J. Damha, *J. Am. Chem. Soc.*, 2003, **125**, 654–661.

7 (*a*) P. Nielsen, L. H. Dreiøe and J. Wengel, *Bioorg. Med. Chem. Lett.*, 1995, **3**, 19–28; (*b*) A. Pasternak and J. Wengel, *Nucleic Acids Res.*, 2010, **38**, 6697–6706.

8 (*a*) D. M. Kenski, A. J. Cooper, J. J. Li, A. T. Willingham, H. J. Haringsma, T. A. Young, N. A. Kuklin, J. J. Jones, M. T. Cancilla and D. R. McMasters, *Nucleic Acids Res.*, 2010, **38**, 660–671; (*b*) N. Vaish, F. Chen, S. Seth, K. Fosnaugh, Y. Liu, R. Adami, T. Brown, Y. Chen, P. Harvie and R. Johns, *Nucleic Acids Res.*, 2011, **39**, 1823–1832; (*c*) J. B. Bramsen, M. B. Laursen, A. F. Nielsen, T. B. Hansen, C. Bus, N. Langkjær, B. R. Babu, T. Højland, M. Abramov and A. Van Aerschot, *Nucleic Acids Res.*, 2009, **37**, 2867–2881.

9 K. C. Schneider and S. A. Benner, *J. Am. Chem. Soc.*, 1990, **112**, 453–455.

10 Y. Merle, E. Bonneil, L. Merle, J. Ságі and A. Szemzö, *Int. J. Biol. Macromol.*, 1995, **17**, 239–246.

11 (*a*) L. Zhang, A. Peritz and E. Meggers, *J. Am. Chem. Soc.*, 2005, **127**, 4174–4175; (*b*) E. Meggers, L. Zhang, A. E. Peritz and P. J. Carroll, *Synthesis*, 2006, 645–653.

12 M. K. Schlegel, X. Xie, L. Zhang and E. Meggers, *Angew. Chem., Int. Ed.*, 2009, **48**, 960–963.

13 M. K. Schlegel, L.-O. Essen and E. Meggers, *Chem. Commun.*, 2010, **46**, 1094–1096.

14 (*a*) H. Asanuma, T. Toda, K. Murayama, X. Liang and H. Kashida, *J. Am. Chem. Soc.*, 2010, **132**, 14702–14703; (*b*) H. Kashida, K. Murayama, T. Toda and H. Asanuma, *Angew. Chem., Int. Ed.*, 2011, **123**, 1321–1324.

15 P. Devarajan, J. J. Johnston, S. S. Ginsberg, H. E. Van Wart and N. Berliner, *J. Biol. Chem.*, 1992, **267**, 25228–25232.

16 (*a*) L. C. Bock, L. C. Griffin, J. A. Latham, E. H. Vermaas and J. J. Toole, *Nature*, 1992, **355**, 564–566; (*b*) R. F. Macaya, P. Schultze, F. W. Smith, J. A. Roe and J. Feigon, *Proc. Natl. Acad. Sci. U. S. A.*, 1993, **90**, 3745–3749; (*c*) K. Padmanabhan, K. P. Padmanabhan, J. D. Ferrara, J. E. Sadler and A. Tulinsky, *J. Biol. Chem.*, 1993, **268**, 17651–17654.

17 V. Kumar, K. R. Gore, P. I. Pradeepkumar and V. Kesavan, *Org. Biomol. Chem.*, 2013, **11**, 5853–5865.

18 (*a*) K. Y. Wang, S. McCurdy, R. G. Shea, S. Swaminathan and P. H. Bolton, *Biochemistry*, 1993, **32**, 1899–1904; (*b*) W. O Tucker, K. T. Shum and J. A. Tanner, *Curr. Pharm. Des.*, 2012, **18**, 2014–2026; (*c*) I. Russo Krauss, A. Merlino, A. Randazzo, E. Novellino, L. Mazzarella and F. Sica, *Nucleic Acids Res.*, 2012, **40**, 8119–8128.

19 (*a*) A. Pasternak, F. J. Hernandez, L. M. Rasmussen, B. Vester and J. Wengel, *Nucleic Acids Res.*, 2011, **39**, 1155–1164; (*b*) T. Coppola, M. Varra, G. Oliviero, A. Galeone, G. D'Isa, L. Mayol, E. Morelli, M. R. Bucci, V. Vellecco, G. Cirino and N. Borbone, *Bioorg. Med. Chem.*, 2008, **16**, 8244–8253.

